THE UNIVERSITY OF ALBERTA

RELEASE FORM

NAME OF AUTHOR RICHARD W. DESAULNIERS

TITLE OF THESIS ELECTRICAL BREAKDOWN IN IONIZED GASES

DEGREE FOR WHICH THESIS WAS PRESENTED MASTER OF SCIENCE

YEAR THIS DEGREE GRANTED 1978

THE UNIVERSITY OF ALBERTA

ELECTRICAL BREAKDOWN IN IONIZED GASES

by

(C) R. W. DESAULNIERS

A THESIS

SUBMITTED TO THE FACULTY OF GRADUATE STUDIES AND RESEARCH

IN PARTIAL FULFILLMENT OF THE REQUIREMENTS FOR THE DEGREE

OF MASTER OF SCIENCE

ELECTRICAL ENGINEERING

EDMONTON, ALBERTA

FALL, 1978

THE UNIVERSITY OF ALBERTA

FACULTY OF GRADUATE STUDIES AND RESEARCH

The undersigned certify that they have read, and recommend to the Faculty of Graduate Studies and Research, for acceptance, a thesis entitled

HIGH VOLTAGE BREAKDOWN IN AN IONIZED GAS

submitted by RICHARD W DESAULNIERS

in partial fulfilment of the requirements for the degree of

MASTER OF SCIENCE

ELECTRICAL ENGINEERING

ABSTRACT

Voltage breakdown in a gas may be either dielectric or thermal in nature depending on the conductivity of the gas. The former occurs during a short time interval ($<10^{-7}$ sec) while the latter occurs over a longer time interval ($>10^{-7}$ sec). The dependence of voltage collapse on plasma density is explored as well as the time required for breakdown. The effect of electrode separation on breakdown and the current-voltage characteristics of the plasma is discussed. The experimental work described here is the study of the behavior of voltages (2-8kV) in a slightly ionized gas, such as is found in a flame. The current voltage characteristics during breakdown are examined and the probable breakdown mechanisms are identified.

ACKNOWLEDGMENT

I would like to thank my supervisor Dr. Peter Smy for his constant encouragment and help in completing my thesis. I would also like to thank the University of Alberta whose financial assistance made it possible for me to complete my Graduate Studies.

TABLE OF CONTENTS

LIST OF TABLES

LIST OF FIGURES

CHAPTER I

INTRODUCTION

1.1 Breakdown in hot gases

In alternating current circuit interrupting devices the post arc period is of paramount importance. During this period the device undergoes a process which determines whether it will or will not perform the duty required. Interruption of current imposes a fairly large transient voltage across the gap and may re-establish the arc. Some authors have speculated that after " current-zero ", breakdown is dielectric in nature while others have postulated thermal breakdown in the case where the electrical conductivity is reasonably high.

Jones[9] has shown that air which is un-ionized follows the well known Townsend relations for predicting voltage breakdown. His experiments were conducted using sparking potentials of 12 to 30 kV and values of pd from 300 to 760 torr cm (where p is the pressure and d is the electrode separation).

1.2 Previous experiments

Some experimental work has been done on the electrical breakdown of high temperature gases by Lee, et al. [12], Sharbaugh, et al. [21] and Mikoshiba[17] using a shock tube to generate the ionized gas. In Sharbaugh's paper he notes that preliminary results indicate that above 2000 K there is a noticeable departure from Paschen's Law. It was also observed that at higher temperatures, corresponding to electron densities in the range of 10^{15} cm^{-3}, the breakdown process undergoes a transition from a rapid to a much slower voltage collapse. This was also observed to occur during voltage breakdown in a flame.

Previous work by Clements and Smy[3,4] has shown that plasma effects are significant at normal flame velocities. Theoretical relationships for thick and thin sheaths have been derived by Clements and Smy[3,4], and have shown good agreement with their experiment. In this experiment it was observed that the slight ionization present in the flame was sufficient to alter the behaviour of a discharge across a gap.

The purpose of the work described here is to study the deviation of the breakdown voltage in an ionized gas from Paschen's law. Paschen's law states that there is a dependency of the breakdown voltage on pd. In this experiment pd (p is pressure and d probe separation)

remains constant but Paschen's law does not account for deviations of the breakdown voltage due to ionization. Originally the experiment was to have been conducted at low pressures (0.5-5 torr) in a shock tube. For various reasons (see Chapter 2) this approach was abandoned and the experiment was finally conducted using a flame plasma.

CHAPTER II

GENERATING THE PLASMA

Initially, the ionized gas required for the experiment generated using a shock tube. This was ideal since the gas in this case was heated through compression by a shock front rather than by exothermic chemical combustion as in a flame. This method of ion production using the shock front had the advantage of not creating complex compositions of ions in the test gas and heated the gas to higher temperatures than possible with a flame alone. Any breakdown characteristics observed then could be attributed to the test gas itself rather than to a hydrocarbon mixture as in a flame. It would be desirable to also determine the effects of high velocity gas flow on breakdown. The shock tube will now be described and the reason given as to why it was finally rejected as a plasma source.

2.1 Shock Tube

The properties of the shock tube are fairly well understood and the basic equations that describe the behaviour of shocked gas have been analyzed and discussed in works done by Simpson[23], Mikoshiba[17], Rose and Camm[1], Resler *et al.* [20] and Gross[8].

A typical shock tube (Fig. 1) consists of two sections, a downstream section at a pressure of p_1 and a driver at pressure of p_4.

The simplified diagram of the shock tube in Figure 1 shows the existing conditions in the shock tube both before and after the initiation of the shock wave. Region 1 refers to undisturbed gas in the downstream section, region 2 refers to the region immediately after the shock wave up to the contact surface. The contact surface refers to the interface where the gas from the driver and the gas of the downstream section are in contact. Region 3 refers to the rarefaction wave expanding back from the contact surface into the driver and region 4 refers to the undisturbed driver gas.

If one considers a frame of reference moving with the shock wave at velocity U then the following equations describe the shock front, where subscript 1 refers to the preshocked gas and subscript 2 refers to the postshocked gas.

1) conservation of mass

$$\rho_1 U = \rho_2 (U - u) = m \qquad (1)$$

where U is the velocity of shock front

u_2 is the gas velocity behind shock front

m is the mass swept up by the shock

ρ is the density of the gas

2) Newton's 2nd law of motion

$$mu_2 = p_2 - p_1 \qquad (2)$$

where p is the pressure

3) Law of Conservation of Energy

$$p_1 U + mE_1 + mU^2 = p_2(U-u_2) + mE_2 + m(U-u_2)^2 \qquad (3)$$

where E is the internal energy of the gas

The three preceding equations are known as the Rankine Hugoniot Equations.

It must be emphasized that these equations are for the ideal gas case only and do not account for effects such as viscosity of the gas, the boundary layer and turbulence. The effects are small enough at low shock speed so that the solution of the Rankine Hugoniot equations will give a fairly accurate description of the behaviour of shocked gases.

As the shock speed increases (M>3) not only do the effects mentioned earlier come into play but ionization and variations in heat capacity complicate the solution of the equations. Mikoshiba[16] used some of Saha's equations (Saha[21] p. 671) and has tried to incorporate some effects of ionization into his solutions. Simpson[23], Mikoshiba[17],

Rose and Camm[1] and Resler[20] have used these equations along with appropriate boundary conditions between the different regions in the shock tube together with some elementary thermodynamic relations of ideal gases to obtain a solution. The asymptotic limit obtained by manipulating the equations is:

$$M = \frac{\gamma_1 + 1}{\gamma_4 - 1} \frac{C_4}{C_1} \qquad (4)$$

where C is the sound speed in the gas

γ is the gas ratio

M is the Mach number

From the above equation it is obvious that for a pressure driven shock tube (i.e. where the shock generated is due to a large pressure differential across the diaphragm and the diaphragm is burst by some means) there exists an upper limit for the shock speed assuming one has an ideal gas. Using air in the driver (γ =1.4, C=344 m sec^{-1} at 300 K) and argon downstream at 5 torr (γ =1.6, C=321 m sec^{-1} at 300 K) the limiting shock speed is M=27.

A few trial runs with the driver pressure at 4000 torr and the argon downstream at 5 torr produced shock velocities of the order of M=3. Pressure transducers were used to detect the passage of the shock front. No detectable signal was produced using a floating Langmuir

double probe, indicating that ionization was not present.

Some of the reasons for the large difference between the experimental and theoretical values are; limitation in shock speed caused by laminar boundary flow, improper rupture of the diaphragm leading to turbulent flow, nonuniform shock structure and variation of the gas properties due to shock heating.

2.2 Electrothermal Shocktube

While equation (4) may not be an accurate representation of the shock speed it does indicate that the factor limiting the shock speed is the ratio C_4/C_1, where C_4 is the sound speed in the driver gas and C_1 the sound speed in the downstream gas. An electrical discharge, by heating the driver gas, increases its sound speed and therefore increases the shock speed.

In the experiment various mixtures were used to produce the shock front:

1) helium driver with air downstream
2) air driver with air downstream
3) air driver with argon downstream
4) air driver with sulfur hexafluoride downstream

The basic arrangment for the electrothermal shocktube

is shown in Figure 1. In the diagram the main capacitor bank C1 was initially charged to a high voltage (8-16kV) and then discharged across the spark gap in the driver. The discharge was initiated by means of a plasma jet injected across the electrode gap of the driver. This resulted in a ringing discharge with a decay time of approximately 100 μsec at a frequency of 47 kHz. Calculations from the voltage-current traces of the discharge indicated that it was highly efficient (50%).

The shock tube system was composed of a driver with an inside diameter of 7.6 cm enclosing a volume of 349 cm^3. A Mylar film approximately 1 mil thick was used as the diaphragm and was held between the flange surface of the driver and the downstream section with two clamps. By using two O-rings of different diameter, one for each flange, the Mylar was gripped with sufficient force to prevent any leaking. This was the thinnest Mylar which could used for a driver pressure of 4 atmospheres with a downstream pressure of one torr.

The downstream section of the shock tube was composed of a 30 cm section of 5.1 cm inside diameter Pyrex tubing, a 35 cm test section, a one meter length of metal tubing and finally a dump tank to dissipate the shock wave. The dump tank was connected to an Edwards High Vacuum Pump Model ED250.

The test section was located aproximately 50 cm downstream and consisted of a thick plexiglass tube with an inside diameter of 5.1 cm. Two sets of cylindrical brass double probes, 0.95 cm in diameter and with a hemispherical tip, were located 10 cm apart at the end furthest from the driver. The two probes in each set were placed diametrically opposite to each other and extended approximately 1.3 cm from the inside wall into the shock tube. They were used to obtain a record of the speed of the shock front and to obtain breakdown measurements. In front of the first set of double probes a thin wire was placed to detect the arrival of the shock front.

The system was sufficiently vacuum tight to be pumped down to a minimum of 0.05 torr. The pressure in the downstream section was measured using two Edwards mercury manometers (0.01-10 torr and 0.001-1.0 torr). Once the downstream section had been pumped down as low as possible (0.05 torr), the test gas was bled into the downstream section (by means of a needle valve located near the driver) at a rate such that the desired downstream pressure of the test gas was obtained. Pumping was continued as the test gas was bled continuously into the shock tube to obtain good gas purity.

Since the sound speed in the driver increases with a

decrease in the driver gas density, thereby resulting in a stronger shock, helium would have been the ideal candidate for a driver gas. At one atmosphere, helium was found to be unsatisfactory as a driver gas due to its low breakdown voltage (8 kV). Pressurizing the driver to 3 atmospheres did not increase the breakdown voltage sufficiently to allow helium to be used as the driver gas. Hereafter air was used as the driver gas since it was capable of holding off the high voltages required without breaking down.

Initially, to test the equipment, air was used in the downstream section. One of the problems caused by the driver section was the large amount of electromagnetic interference generated during the process of discharging the capacitors across the driver gap. This interference was picked up by the oscilloscope and other sensitive pieces of equipment causing spurious false triggering.

In an attempt to eliminate the effect, high speed grounds were installed but to no avail. Another method was attempted by which a voltage divider network was used at the input to attenuate the inteference picked up at the input. The input trigger pulse was increased to compensate for the attenuation. It however proved to be unsuccessful in decreasing the sensitivity of the ramp trigger.

The final solution adopted was a combination of

digital and delay circuits (Fig. 2) to lock out any inteference from the trigger probe to the ramp generator (Fig. A1) until the inteference from the driver discharge had dissappeared. This proved to be a successful method for eliminating the inteference.

The time required for the shock to reach the probes was long enough after the discharge that no interference from the discharge was noticeable. While this system was workable further experimentation proved to be unfruitful as will be explained later on.

Using argon as the downstream gas, an attempt was made to calibrate the shock tube by comparing it to previous experiments. Various pressures (1,2 and 4 torrs) of downstream gas were used. The speed of the shock front was measured by calculating the difference in arrival time at the two succeeding sets of probes. The oscilloscope signal was obtained by putting a 45 volt battery in series with a 10 kΩ resistor and the probe as shown in Figure 1. The arrival of the ionizing shock front resulted in a decrease in resistance of the downstream gas which caused an increase of current flowing through the 10 kΩ resistor thus producing a detectable signal.

A trace of the typical signals obtained from the two sets of floating double probes are shown in Figures 3a and

3b. From the typical traces of the two probes as shown in Figure 3a one can calculate from the difference in arrival time the shock speed. Figure 3a was a typical trace of a signal that one would obtain as a result of turbulent mixing behind the shock front.

Figure 3b is a typical trace of the desired signal which would occur at either probe. It usually consisted of an initial rise in voltage followed by a slight decrease then another rise in voltage. The first increase was probably due to the shock waves ionizing the gas. Even though the shock front was fairly thin ($<10^{-6}$ cm, Greene[7]), the conductivity relaxation time of the gas caused the voltage to rise more slowly than the pressure across the shock front. The second increase in Figure 3b was due to the arrival of the heated gas of the driver. The interval between the two increases was about 30-40 μsec.

The occurence of either Figure 3a or 3b was random and could be attributed to the non-reproducable bursting characteristics of the diaphragm.

Results of the measurements of the shock speed for various driver voltages and downstream pressures are shown in Figure 4. The shock speed increases linearly with the driver voltage as expected but tapered off above a certain shock speed at high downstream pressures. Any further

increase in the amount of energy dumped into the driver failed to increase the shock speed. This was due to the high levels of ionization absorbing energy from the shock front thereby preventing any further increase in shock speed.

Assuming that the free electrons and argon ions are in thermal equilibrium with the argon atoms behind the shock wave, Mikoshiba[17] calculated using Saha's equations (Saha[21] p.671) a simple result from statistical mechanics.

$$\alpha^2 = \frac{1}{340\, p\, T^{5/2}\, e^{1.82 \times 10^5 / T} + 1} \qquad (5)$$

where α is the fractional ionization

T is the gas temperature in K

p is the gas pressure in torrs

e is 2.718...

Assuming a temperature of 8000 K for the gas at the recorded shock speed (M=8) (see Resler[20]) the calculated ionization level was approximately 5%.

Except for an occasional unpredictable result, the shock speed reproducibility was consistently within 10%. Some of the possible reasons for the fluctuation in measurements are:

1) non-uniformity of the gas flow caused by the boundary layer and non-uniform driver discharge
2) inaccuracies in curve interpretation
3) reflection and refraction at the joints between the sections of the shock tube

By comparison with results obtained by Camm[1], the signals from the probe measurement of the shock front seem to indicate a highly irregular contact zone. Using high speed image converters in conjunction with measurements, Camm was able to detect turbulent mixing up to the shock front in some cases. Such runs were attributed to poor diaphragm rupture.

One of the shock tube experiments that would have been performed was using sulfur hexafluoride (SF_6) as the test gas in the downstream section of the shock tube. SF_6 is used extensively as an insulator in high voltage current interrupting devices due to its electron absorbing properties. One of the methods used to extinguish an arc once the contacts are opened is to blow a jet of SF_6 gas in the gap. In the shock tube it would have been possible to study the effects of hypersonic gas flow on breakdown.

Preliminary testing indicated that SF_6 had a high resistance to being ionized. This was due to the small

range of energies available for generating the ionizing shock wave and the electron absorbing properties of SF_6. The conductivity of the ionized gas did however vary over a few orders of magnitude. This lack of cosistent reproducibility and the highly turbulent nature of the test gas made any further testing unproductive.

The design of the shock tube was limited by the machining techniques available at the time which were inadequate for the purpose of this experiment. The inside wall of the shock tube could not be machined smooth enough and no techniques were available for polishing it. It would have been desirable to fabricate the length of the shock tube from the driver up to the probes from one seamless tube. A longer tube would be necessary to assure a sufficient separation between the shock front and the contact zone. A more energetic driver discharge to enable a higher downstream pressure to be used and more sophisticated diagnostics would have been required to obtain worthwhile results.

CHAPTER III

EXPERIMENT

3.1 The flame

Since the flame was the most suitable and reproducible source of ions, all the following measurements for the high voltage breakdown experiment used the flame as the ion source.

The burner used in this experiment is known as a Meeker burner. In this type of burner the flow velocity is balanced against a burning velocity essentially unaltered by heat losses to any solid body so as to produce a relatively flat flame perpendicular to the flow direction. The approach stream was first made uniform by an assembly of randomly distributed obstacles consisting of fine grids and screens. In Lawton[11] it was stated that the thickness of the reaction zone at atmospheric pressure varies from a maximum of 3 mm, for near flame limits, to very small fractions of a millimetre for stoichiometric mixtures. Because of the mixing caused by the screens the reaction zone was not well defined, but occured across the diameter of the mouth of the Meeker burner.

3.2 Flame experiment

3.2.1 Diagnostic equipment

The diagnostic equipment, as shown in Figure 5, consisted of a Tektronix 556 dual beam oscilloscope with two 1A5 differential amplifier plug-in units.

The signal leads from the Tektronix High Voltage Probes (P6015) 1 and 2 were connected to the differential input of an oscilloscope channel unit to obtain the voltage across the double probe. The signal across the resistor R was picked up by probe 2 and amplified by the other unit to obtain the current. Since the double probe was in series with the grounded resistor R, the current flowing through the probe could be calculated easily from the voltage drop across R .

While the 1A5 unit had a wide frequency response (up to 10 MHz), its sensitivity was limited to about 1 mV (this being equivalent to 1 mA for this experiment). The Tektronix probes were calibrated and balanced using the ocilloscope. Their frequency response was greater than 10 MHz.

All the dc measurements were made using the 1A7 differential amplifier unit. Its variable bandwidth was set at dc up to 1 kHz to eliminate as much external

interference as possible. One source of such interference that still remained was the 60 Hz signal from the power lines. By splitting the input signal into the two inputs of the differential amplifier, one set to dc and the other set to ac and inverted, most of the 60 Hz signal was eliminated leaving only the dc component.

Both photographic and visual observation were used to obtain the data. For dc measurements a high voltage dc supply was used (0 -- 12kV at 10mA). For the transient measurements a camera combined with a simple ramp voltage generator, as explained in the appendix, was used to obtain the experimental data.

3.2.2 Double probe

The double probe was constructed from two lengths of standard brass tubing 0.16 cm in diameter bent into a semicircle with a 0.5 cm radius. This was the smallest radius the tubing could be bent into without severely kinking the tubing. Each probe had a surface area of 0.03 cm^2 exposed to the flame.

The probes were mounted on teflon insulators to electrically isolate them from the apparatus and were then connected with Polyflow tubing to a compressed air supply for cooling. If the probes were not cooled it was found

that the conduction was enhanced by thermionic emission from the probe surface.

Though Loeb[14] in his text states that oxides on the electrode surface and electrode roughness most certainly affect the sparking, this was not considered an important parameter of the experiment since the current-voltage characteristics of breakdown under the worst case conditions, such as would be found in circuit breakers, was under study for this experiment. In fact Jones[9] states that surface roughness greatly enhanced electron emmision from the cathode under an electric field. But on the other hand the oxide film can decrease the effect of the photoelectric bombardment of the cathode. From Meek[15], and Penning[18] though, it was stated that the breakdown voltage was independent of the probe material at high enough pressures.

3.2.3 Conductivity measurements

There is a very great advantage to be gained from using two probes of comparable area when measuring electron temperature since the electron current to either one of them cannot exceed the sum of the positive ion currents to both. It is also essential that the current taken by the probe should be small compared to the rate of ion generation in the plasma under study. But the double probe

could not be used effectively in this experiment to measure ion density, since two other conditions had to be fulfilled. The voltage across the probe had to be kept small and the probe had to have a well defined geometry for accurate measurment (ie. planar, cylindrical or spherical).

In the case of the flame, additional difficulties may have risen due to chemical, thermal and aerodynamic disturbances of the reaction processes by the probes. Rates of free charge generation could also have been measured using the saturation current technique.

In principle then, it is possible to measure flame ion concentration from the currents withdrawn in terms of conductivity. Since the concentrations are the results of competition between the rate of generation and the rate of recombination, perhaps this was not the most accurate method of measuring flame ion concentration (particularly since both these rates vary rapidly with position in the flame and all the possible methods of recombination and generation average out over appreciable distances). The conductivity of the flame will be discussed in section 3.3.

3.2.4 Flame

In normal hydrocarbon flames, as many as ten product species occur in the dissociation process. By using the

dissociation equilibrium constants as well as other thermodynamic data as required, the composition can be determined at various temperatures. The method was cumbersome rather than difficult. With the flame temperatures and ionization potentials involved, however, the extent of thermal ionization was not high enough for an appreciable part of the energy to be tied up in that form.

Initially (Sec 3.3), an attempt was made to determine the dependence of the probe current and voltage breakdown on the variations in probe separation by using a mixture ratio of 9.36 cm^3 sec^{-1} propane and 110.1 cm^3 sec^{-1} air.

Various mix ratios were then tried with the probe separation set at 0.5 cm. The different mixes were obtained by varying the propane flow meter (100%=26.7 $cm^3 sec^{-1}$) and the air flow meter (100%=314.6 $cm^3 sec^{-1}$). The mixes that were tried are summarized in Table 1. In the table, F refers to the flow rate in cm^3 sec^{-1} where the subscript A refers to primary air and the subscript P refers to propane. By varing the mixture ratios, different rates of ion production and therefore different ion densities can be obtained.

During the course of the experiment it was found that there was a maximum flow rate where the flame became unstable and then extinguished itself. This situation is

known as blow-off and was a result of the flow rate being larger than the velocity of the combustion zone.

Table 1. Flow rates and mix ratios of air and propane.

F_A $cm^3\ sec^{-1}$	F_P $cm^3\ sec^{-1}$	F_A/F_P	F_A+F_P $cm^3\ sec^{-1}$
110.1	9.36	11.8	119.5
110.1	12.0	9.18	122.1
110.1	14.7	7.49	124.8
141.6	9.36	13.6	151.0
141.6	12.0	11.8	153.6
141.6	14.7	9.63	156.3
173.0	9.36	18.5	182.4
173.0	12.0	14.4	185.0
173.0	14.7	11.8	187.7
204.5	9.36	20.3	213.9
204.5	12.0	17.0	216.5
204.5	14.7	13.9	219.2

3.3 dc measurements and breakdown

In the process of obtaining any sparking potential measurement, the potential applied was gradually raised and the passage of a spark was looked for. Unless an electron appeared in the appropriate place in the gap when the potential was reached there would have been no spark. The potential would then have been raised and the potential at which the spark finally appeared might have been considerably above the value at which it would have appeared had electrons been present. That is, the statistical time lag had to be reduced to a time interval less than the time delay between increments of the potential increase. Loeb[14] states that introducing a source that will produce of the order of one electron per microsecond in the active volume of the gap will reduce the fluctuation of the observed sparking potential from a spread of 5% to 10% to less than one percent. By incrementing the voltage increases slowly the fluctuations of the dc breakdown voltage was well below 5% so it was not deemed neccesary to be improved upon.

For the dc measurements the resistance R of the external circuit was set to 537 kΩ. This was to limit the current (<10 mA) from the dc power supply once breakdown had occurrred. The impedance of the flame was large enough so that most of the voltage potential appeared across the

double probe rather than across the limiting resistor prior to breakdown.

The dc current was then measured for different probe spacing by slowly raising the voltage until breakdown occurred. The results were plotted in Figure 6.

The current increased steadily with voltage as expected until just prior to breakdown where it tapered off to a saturation value. Von Engel[25] states that this limiting current j_B is simply that j for which the distribution of space charge causes secondary ionization in the gas at one or both electrodes. j_B here would depend on the probe spacing, since space charge continues to cause the field intensity to increase over the extent of these regions unlike j_S which is a property of the flame alone.

Only small differences in the current were noted for different probe spacing, indicating that perhaps the sheath mechanism was in effect as explained by Clements and Smy[4]. From the value obtained by Smy it would seem to indicate that since the breakdown was greater than 1000 volts the normalized sheath thickness would have been well over 100 (ratio of probe radius to sheath thickness). The sheath thickness then would have been over 8 cm. The curves (Fig. 6) also seemed to show a $V^{1/2}$ dependency as derived by Clement and Smy [3,4].

In both Figure 7 and 8 the breakdown voltage increases with probe separation as expected. The breakdown is considerably below that of air at atmospheric pressure. From one of Von Engel's figures[25] (Fig. 104, p. 99) we can observe the breakdown voltage to be aproximately 10kV for a 0.5 cm gap at one atmosphere.

The transient characteristics of breakdown in the flame were obtained by recording the resulting voltage current variation of the gas between the two probes as the voltage pulse from the ramp generator was applied to the cooled double probe. The external resistor used in this case was 1014 Ω. This allowed the detected signal to be sufficiently large enough to obtain a recording of the current variations and yet the resistance was small enough to allow the transient current to go as high as 5 A.

The breakdown voltage for a pulsed voltage (Fig. 7) is substantially lower than the dc breakdown (Fig. 8). Smy and Clements[3] attribute this to the finite relaxation time of the sheath surrounding the probe. A sudden application of voltage can be expected to result in higher transient sheath electric fields leading to breakdown while a gradual application does not necessarily produce breakdown.

The breakdown time does not seem to be affected by the probe separation. This had been noted by previous

investigators where the overvoltage was substantially higher than the breakdown voltage. In a few cases the breakdown time increased when the breakdown voltage was just less than the overvoltage.

Corresponding dc current-voltage measurements were made for the seeded flame as shown in Figure 9. The conductivity had increased by an order of magnitude but the breakdown voltage seemed to have been only slightly affected. When the ramp voltage was applied across the probes to observe the transitory characteristics of breakdown it was found that the results were unreliable. This was due to the potassium hydroxide deposits on the probe. Clearly a probe that was kept continuously in the flame was less advantageous than one which would have been swept through the seeded flame to prevent deposits.

3.4 Experimemtal Results

One of the interesting results was the different types of progressive increases in current that occurred with the increasing voltage for different mixture ratios as shown by the typical Figures 10a, 10b, 10c.

Figure 10a indicates a typical breakdown in a fuel rich mixture ($F_A/F_P < 14$) while Figure 10b (F_A/F_P 14) and

Figure 10c ($F_A/F_p > 14$) are typical of a breakdown where the primary air has been increased to promote a more complete combustion. In Figures 11 and 12 one can see clearly the dependence of the breakdown voltage and the calculated saturation current on the mixture ratio.

Sharbaugh et al. [22] divided the breakdown mechanism into two categories, "dielectric" and "thermal" breakdown. Thermal breakdown is associated with the fact that the plasma is a sufficiently good electrical conductor to suffer considerable Joule heating, which raises its temperature and hence its conductivity, leading to some form of breakdown.

The second form is "dielectric" breakdown where the applied electric field is distorted to a greater or lesser degree by an electrical sheath formed around the cathode probe due to the presence of ionization. When the voltage gets large enough, the sheath, though limited by the saturation current, will eventually break down. The current will increase to a value usually dictated by the plasma resistance. Finally with increasing voltage another breakdown occurs, which may be thermal, and the spark appears. The breakdown which occurred in this experiment, as discussed in Chapter 4, cannot be explained as being "dielectric" or "thermal".

In Figure 10a the breakdown characteristics are typical for a flame whose mixture was fuel rich. This resulted in an ion poor flame. No increase in current was noticed prior to breakdown. The most probable mechanism of breakdown was "dielectric" breakdown. The current was less than 1 μA and therefore too small to detect using the present instruments.

In Figure 10b two different types of breakdowm occurred. Figure 10b is transitory and evolved from Figure 10a to Figure 10c as the mixture of primary air was increased.

The progressive development into the spark discharge of Figure 10c could be explained in terms of the current-voltage properties which showed a continuous development from Townsend discharge to the spark discharge. These characteristics would not show up in dc measurements since to a large degree the discharge characteristics were highly unstable.

The initial stage for the discharge of Figure 10b was thought to be the usual Townsend discharge where the current ($<10^{-6}$ A) was increasing steadily with voltage, but at 0.6 - 0.8 of the breakdown voltage there was an increase in the current by a few orders of magnitude to a saturation value. This is referred to as the glow or corona

discharge. After this the voltage breakdown occurs and the current increases rapidly until it is limited by the external circuit. This, however, was not observed in all cases.

After the initial steep fall in voltage in the voltage-time characteristics a further drop may occur. In a paper by Haydon[6], and another by Clement and Smy[3], the first voltage drop was identified with the appearance of a diffuse glow discharge (Fig. 10d) and the second with the change to a filamentary spark channel. It was also observed by Haydon[6] that the rate of rise of current depended on the gas pressure.

As seen in Figures 10b and 10c, the current starts from an observable initial value which will be called the saturation current for reasons to be made clear later on.

This saturation current was estimated from the data by curve-fitting the current against time using an exponential curve. From the resulting fit, the exponential rise time and the initial current were derived. Figure 13, 14 and 15 were plotted from the derived values. The current in all cases was the total current to the probe rather than the current density.

In Figure 14 the faster the current risetime the higher the breakdown voltage. Also shown in Figure 13 is

that the lower the saturation current the higher the breakdown voltage. Assuming as Clement and Smy[3] did that the ionization density was proportional to the current and also assuming that the current calculated in Figure 13 was roughly the saturation current before breakdown one can see a logrithmic dependence of breakdown voltage current. This can be related to the logrithmic dependence of voltage on sheath thickness. For thick sheaths the current drawn was proportional to the thickness of the sheath. From the graph it can seen that large changes in current result in only small changes in breakdown voltage. But there seems to be a minimum breakdown voltage (1.2 kV) which was unaffected by any further increase in saturation current. There appears to be no relationship however, between the risetime and the saturation current as shown in Figure 15.

CHAPTER IV

DISCUSSION AND CONCLUSIONS

4.1 Gas Temperature

In the voltage-current characteristics of the discharge there existed a region just before breakdown, where a measureable amount of energy was being dumped into the gas between the probes. If one defines the onset of voltage decrease (Fig. 10) as breakdown, one can calculate, using numerical integration, how much energy was dissipated between the probes just before the voltage collapse.

One can find an upper extreme in temperature increase of the gas for the steady state case by making the following assumptions. The discharge takes place in a cylinder with a diameter equal to the probe diameter (0.16 cm) and a length equal to the probe separation (0.50 cm). The volume of the cylinder was therefore 0.01 cm^3. Since the measurable energy before breakdown was being dumped into the gas over such a short time span ($10^{-5} \rightarrow 10^{-6}$ sec) one can safely assume convective and conduction losses to be minimal.

By assuming a high enough temperature to cause thermal ionization one can predict that even black body radiation heat loss would be minimal compared to the energy that is being dumped in the gap. Therefore one can assume that the discharge process was adiabatic. Using a basic thermodynamic relationship

$$\frac{\Delta U}{\Delta T} = \frac{C_p}{1.4} \qquad (6)$$

where

U is the internal energy (cal gm^{-1})

T is the temperature in K

C_p is the specific heat (cal gm^{-1} K^{-1})

Assume the following properties for air at 2000 C, as derived from the thermodynamic tables:

$C_p = 0.3$ cal gm^{-1}

$\rho = 0.003$ gm cm^{-3}

Taking the largest value for energy from the graph on Figure 16 ($\approx 1.5 \times 10^{-3}$ J) one get an approximate value for the maximum possible temperature rise per unit volume

$$\Delta T = \frac{(1.4)\,\Delta U}{C_p} = 55 \text{ K}$$

Since significant thermal ionization (> 1%) does not occur for temperatures less than 4000 C one can only

conclude that the energy dumped across the gap was not sufficient enough to cause thermal ionization. However the seeming dependence of breakdown voltage on the energy dumped into the gap (Fig. 16) does seem to indicate heating. But as shown by the above calculation the energy dumped into the gap prior to breakdown was, even under ideal conditions, insufficient enough to cause a significant temperature rise thereby precluding any heating of the gas leading to ionization.

Similarly one can do a rough calculation of the maximum number of electrons that could be produced by considering the ionization potential of molecules in air (O_2 =14.5 eV, N_2=15.1 eV, N = 14.5 eV, O =13.5 eV). Assuming the ionization potential to be about 10 eV, 1 mJ of energy could produce aproximately 10^{14} electrons in a volume of 10^{-2} cm^3. This amounts to an electron density of 10^{16} cm^{-3}. One could possibly conclude that nonequilibrium ionization through electron collision is a likely mechanism for incresing the conductivity leading to breakdown.

4.2 Nonequilibrium Ionization

Two different types of nonequilibrium ionization are discussed in the literature. The first type is caused by the increasing potential applied across the probes. Since the electrons were less massive, one would not expect an

electron to have been able to ionize a neutral molecule until it had achieved sufficient kinetic energy. Any collision with the more massive neutral molecule would have involved little transfer of momentum until the electron had been sufficiently accelerated by the electric field between the probes. As the electric field intensity increased, the electron would have been accelerated sufficiently within a collision length to ionize a molecule. This process would have increased the conductivity with increasing voltage. Eventually an electron avalanche would have occurred once the voltage had increased beyond a critical value (see Figs. 10b and 10c).

A second type of nonequilibrium ionization, discussed by Lawton and Weinberg[11], could be the main source of ionization in most flames.

In the case of normal hydrocarbon flames, the nonequilibrium ionization peaks, which are thought to be due to chemi-ionization, give by far the highest concentration of free charge (Lawton[12] p. 226). In a process of this kind the species undergo a chemical rearrangment that releases sufficient energy to ionize one of the products. This seems to be supported by the fact that the saturation current increased as the air/propane mixture increased (Fig. 12). The recombination rate would decrease due to the electron current to the probes. Thus

as the voltage is increased a significant increase in ion production could be expected due to the current withdrawn by the probes.

4.3 Discussion

In work done with plane electrodes, Haydon[6] and Kohrmann[10] identified five regions of current development similar to Figure 10b :

1) $t_o < t < t_1$ immediate post breakdown region for a current extending from 0 to 10 μA
2) $t_1 < t < t_2$ a maximum was observable in some cases. The time scale of this particular region was too small for resolution
3) $t_2 < t < t_3$ diffuse glow discharge or corona discharge where current slowly increases linearly
4) $t_3 < t < t_4$ the filamentary glow region or the prechannel region where a filamentary luminuous channel develops out of the glow discharge column
5) $t_4 < t$ the spark channel formation in the experiment

In a paper by Kohrmann[10], calculations were made in hydrogen for a plane discharge at pd = 1000 torr cm (the experiment here was pd = $10^2 \rightarrow 10^3$ torr cm). Even though

the probes used in the present experiment were cylindrical rather than planar the current and voltage discharge characteristics were observed to be similar to Korman's calculated values.

In the region ($t_1 < t < t_2$) the current was observed to saturate to a maximum. Lawton and Weinberg[12] postulated two possible mechanisms for the current saturation. When the field is applied, the recombination equilibrium is perturbed by the addition of a charge withdrawal term where the ions are being withdrawn by the probe. As the field is increased, the latter competes against recombination with increasing success and the current increases with applied potential. The current then ceases to increase with applied potential, reaching a saturation value, which is the integral of the generation rate across the flame thickness and is independent of electrode separation except for flames of high product ionization. This state persists until the field is high enough for secondary ionization to occur somewhere in the system. Thereafter the current rises with applied potential.

Another limitation in the current drawn which could equally apply (VonEngel[25] see sec 3.3), is current saturation due to space charge effect and is largely independent of the nature of the ion source. The limiting current at breakdown was simply therefore the current for

which the distribution of space charge caused secondary ionization.

Lawton[12] states that since the flow is turbulent in nature due to the premixing and that the small probe diameter would have caused a more intense field at its surface than a plane probe, thereby focusing the current, then space charge may be the dominating mechanism for current saturation.

The observed formative time lag of the spark breakdown in air near atmospheric pressure was so short that the positive ion formed in the gap could not have possibly had time to cross the gap. Thus the Townsend Theory in the case of ionized gases was inadequate near atmospheric pressure and the streamer theory was developed by Loeb[13] and Meek[15] for this pressure region.

4.4 Conclusion

Though the flame has been a subject of research for a long time by such authors as Lawton[11], Loeb[14], Penning[18] and VonEngel[25], to name but a few, the subject is still abundant with possibilities. Though the flame is a relatively cool plasma the process of breakdown cannot be explained in terms of the process that would occur in free air. The breakdown process is not simple and does not have

the characteristics that would identify it as being dielectric or thermal.

A more controlled experiment using cylidrical or plane geometry could determine the dependence of voltage breakdown on conductivity and voltage risetime. Ideally the voltage risetime should be long enough to allow a transient phenomena to die out. The fact that Figure 8 shows a much lower breakdown than Figure 7 suggests that the voltage rise time of the ramp may have been too rapid.

Probably the single most uncontrolable parameter was the plasma source. Under laboratory conditions it is difficult to obtain a "pure" plasma (i.e. one containing just the electrons and ions of the test gas involved). One possible method of generating a source of plasma is use an arc discharge in different gases. In this case the probes would have to be swung through the discharge to prevent heating of the probe.

Another alternative is to blow a jet of high pressure gas through the arc to a set of planar probes. This would simulate more closely the conditions in a circuit breaker. By using a rectangular channel with the opposing wall being either insulators and electrodes a very well defined geometry would be established to study the effect of ionization on breakdown at high pressures. Temperatures as

high as 4000 C could easily be acheived by the arc.

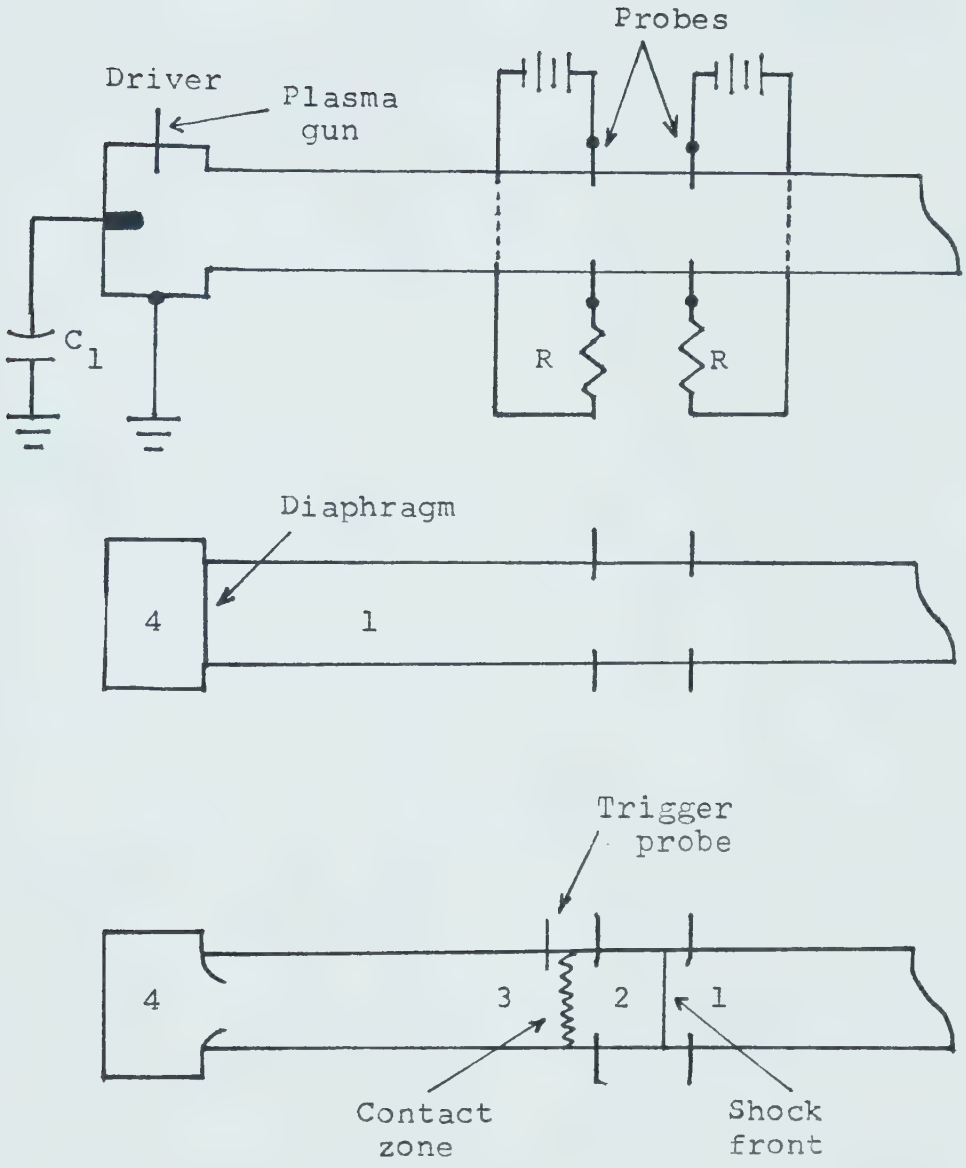

Figure 1. Electrothermal shock tube.

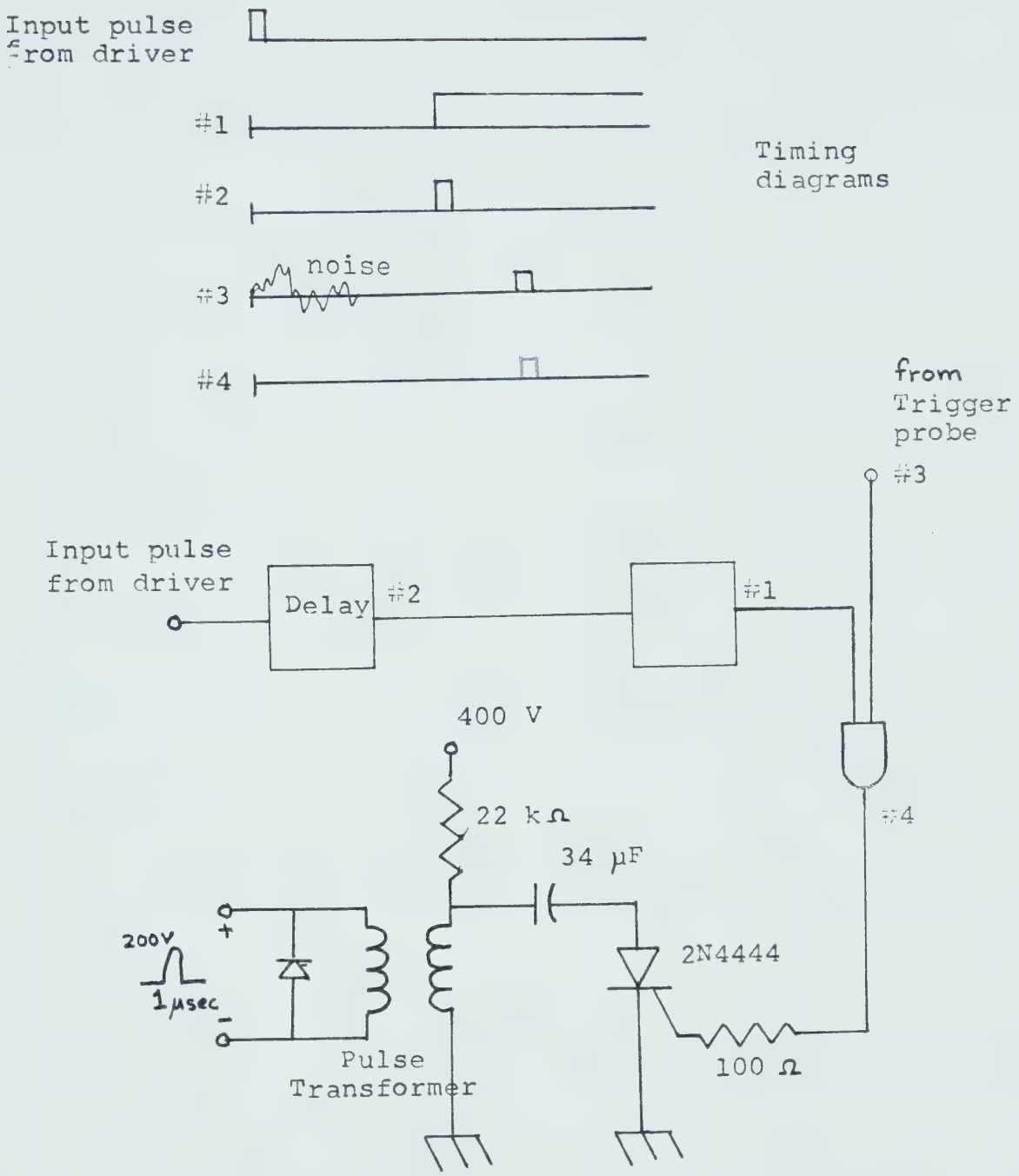

Figure 2. Delay circuit.

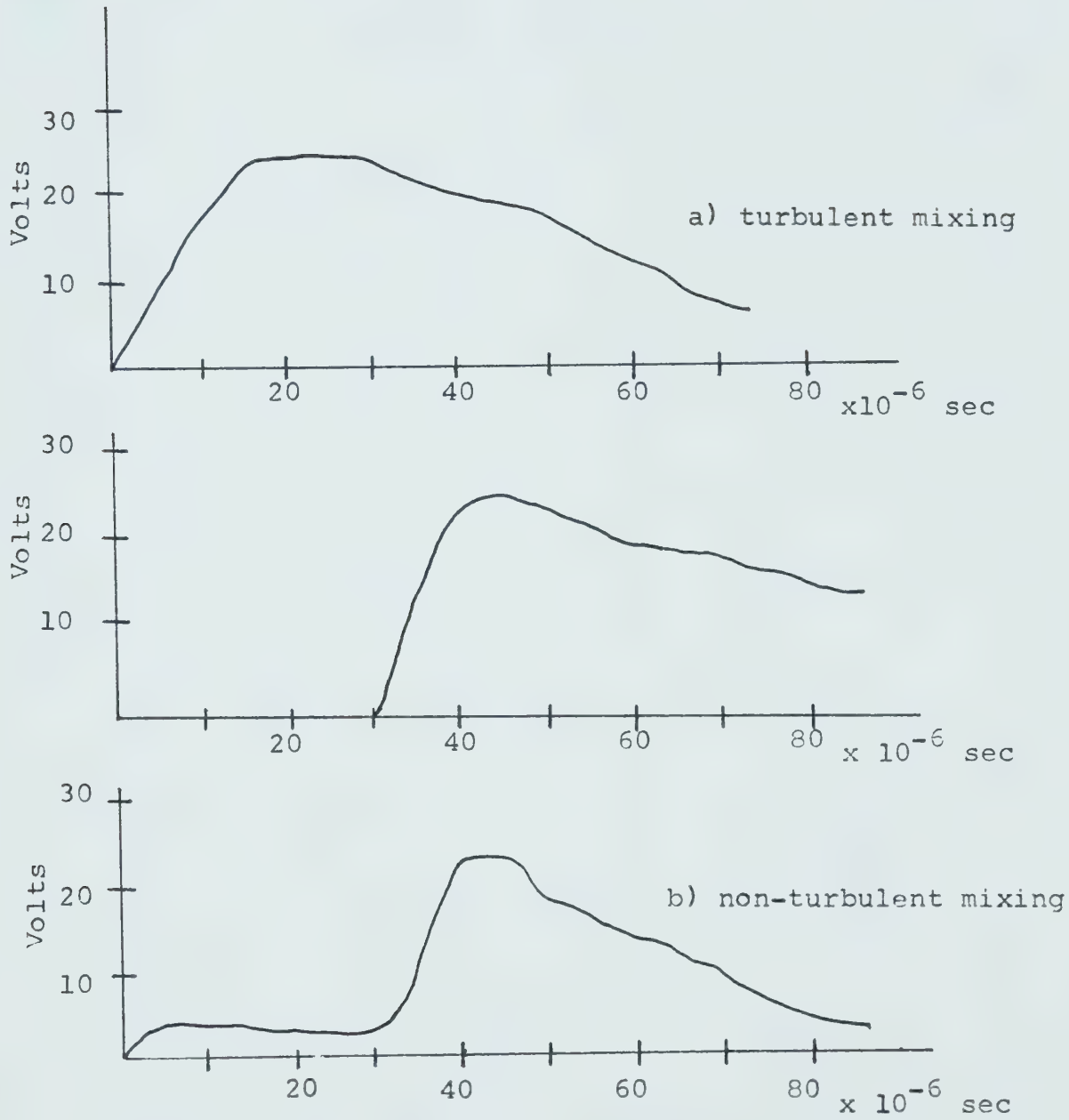

Figure 3. Typical trace of shock front arrival.

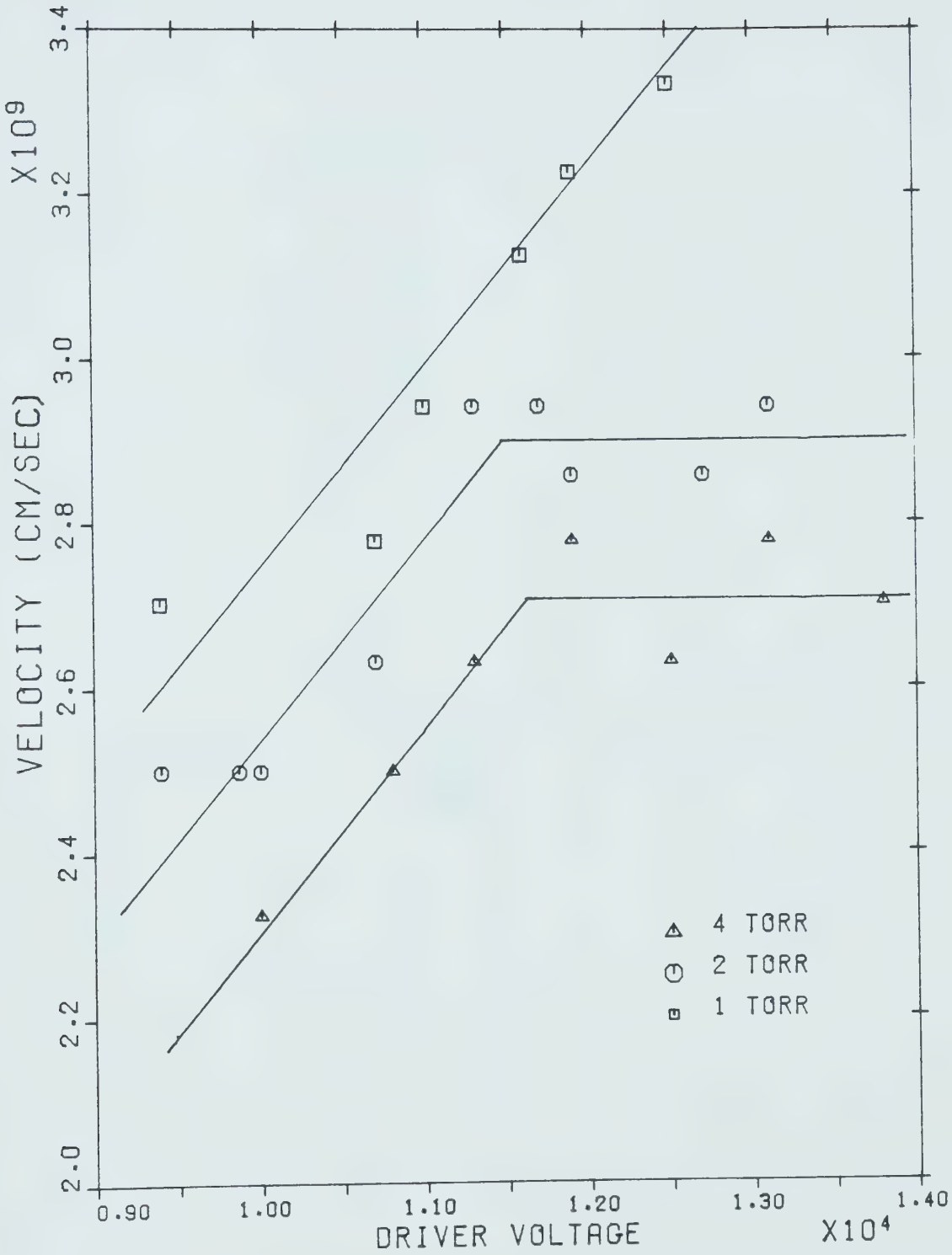

Figure 4. Shock speed versus driver voltage.

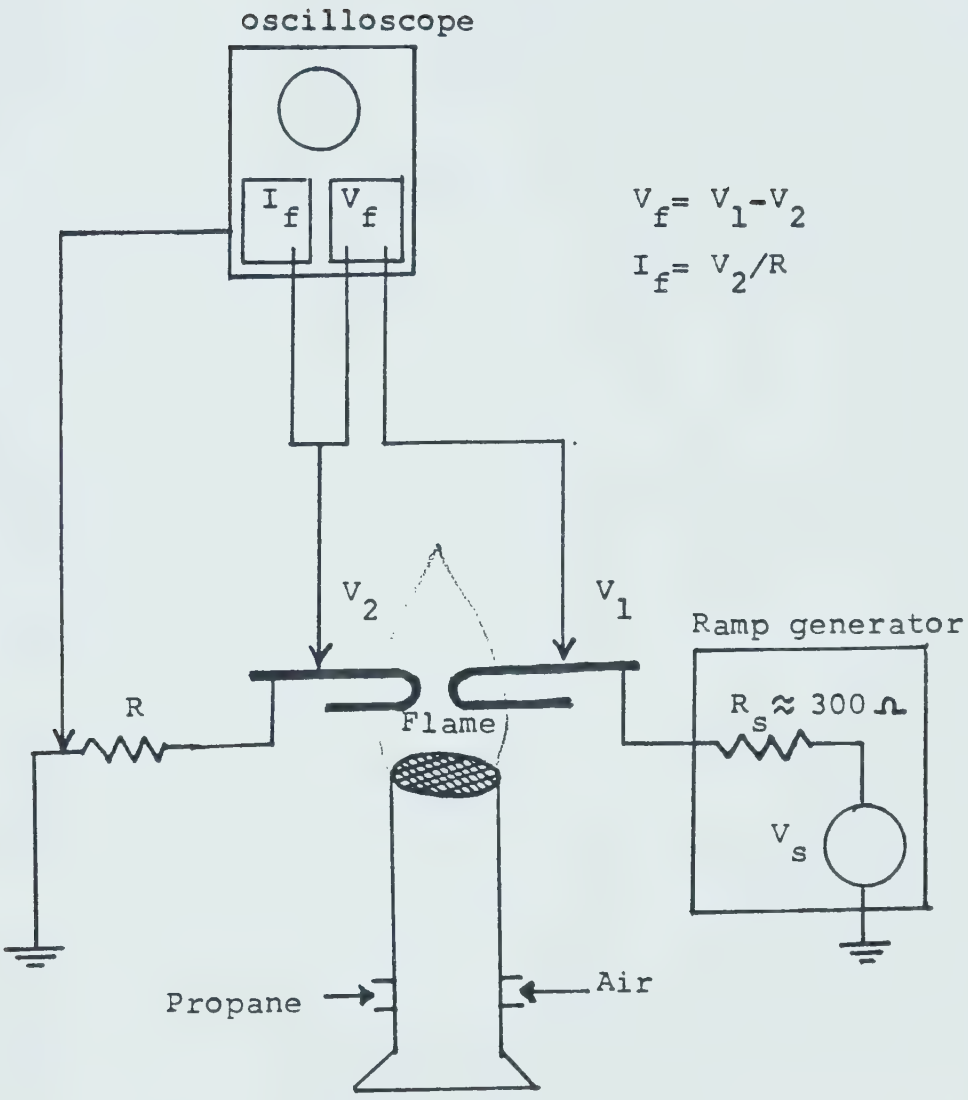

Figure 5. Flame experiment.

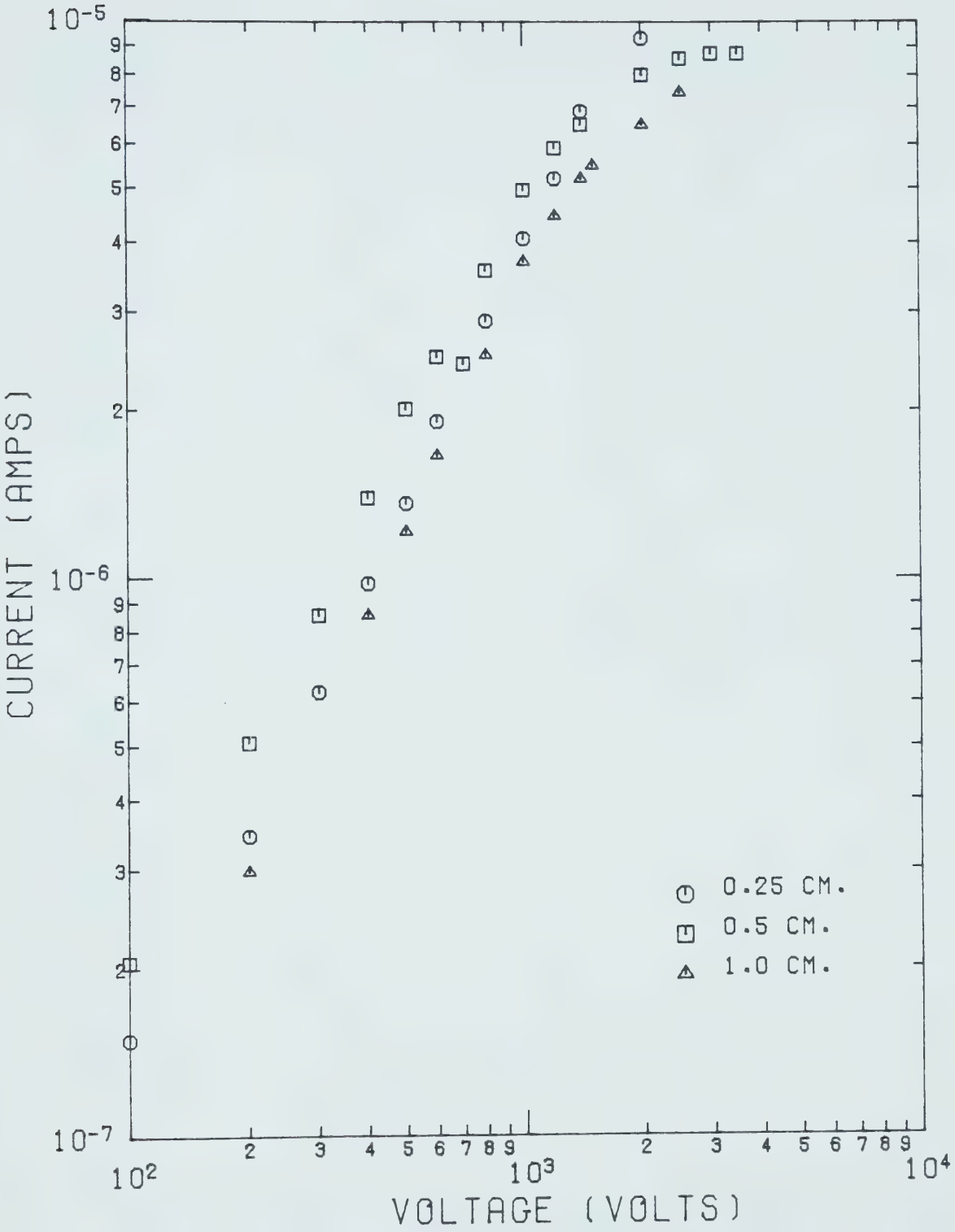

Figure 6. Voltage-current measurments in a flame for different probe spacing with air (110.1 $cm^3\ sec^{-1}$) and Propane mixture (9.36 $cm^3\ sec^{-1}$)

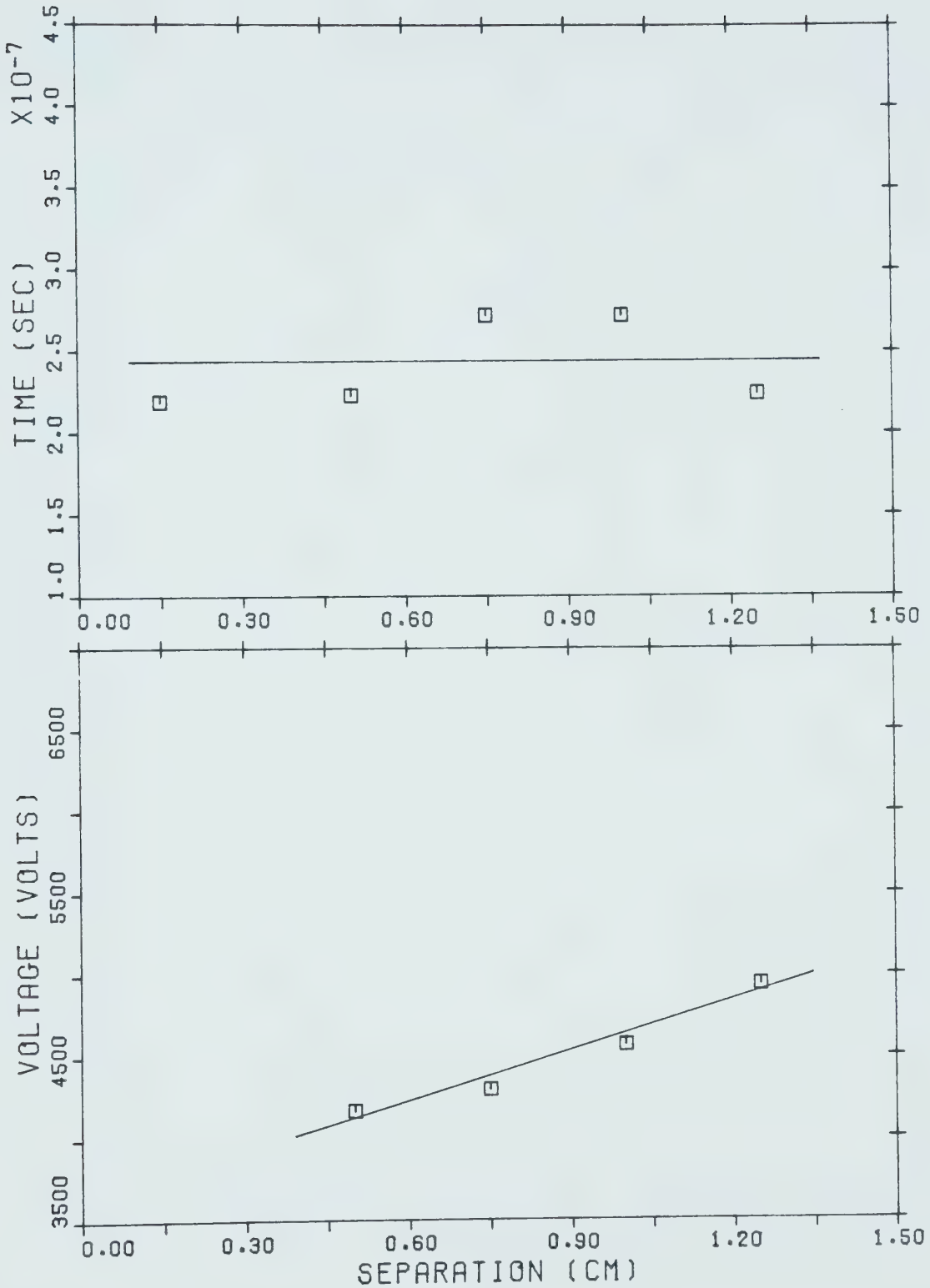

Figure 7. Probe separation versus breakdown voltage and collapse time.

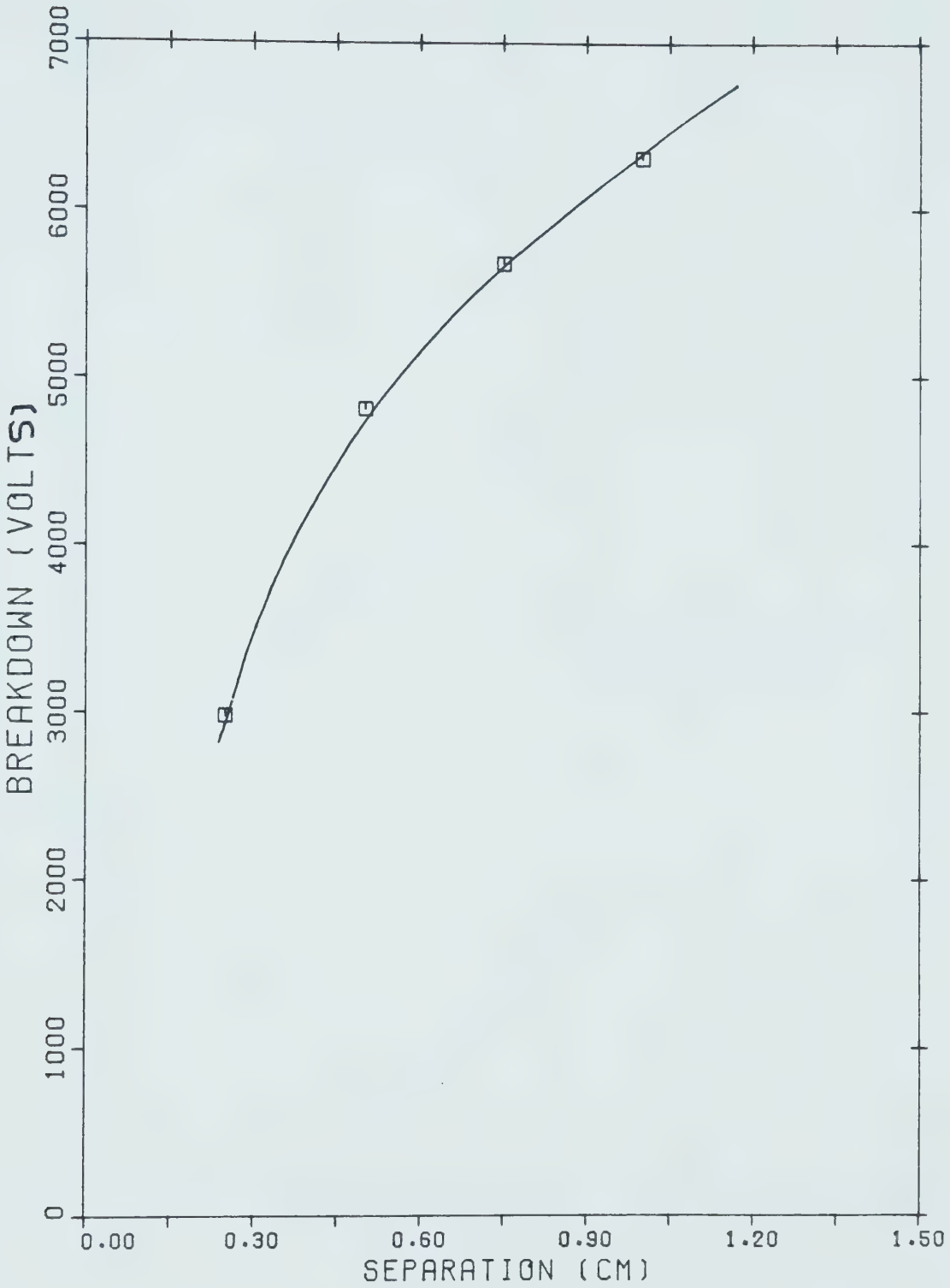

Figure 8. dc voltage breakdown versus probe separation.

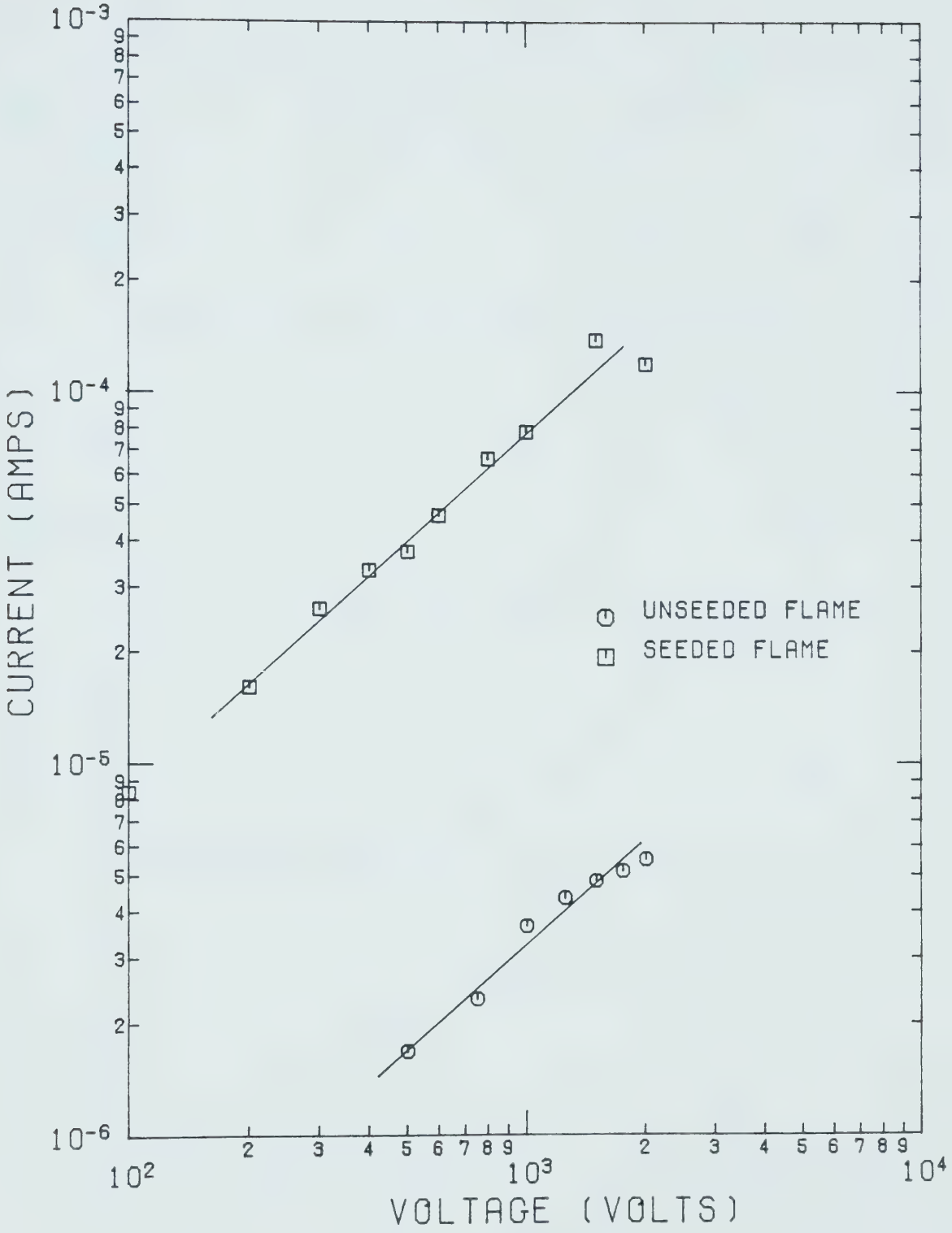

Figure 9. Voltage-current measurement of seeded and unseeded flame.

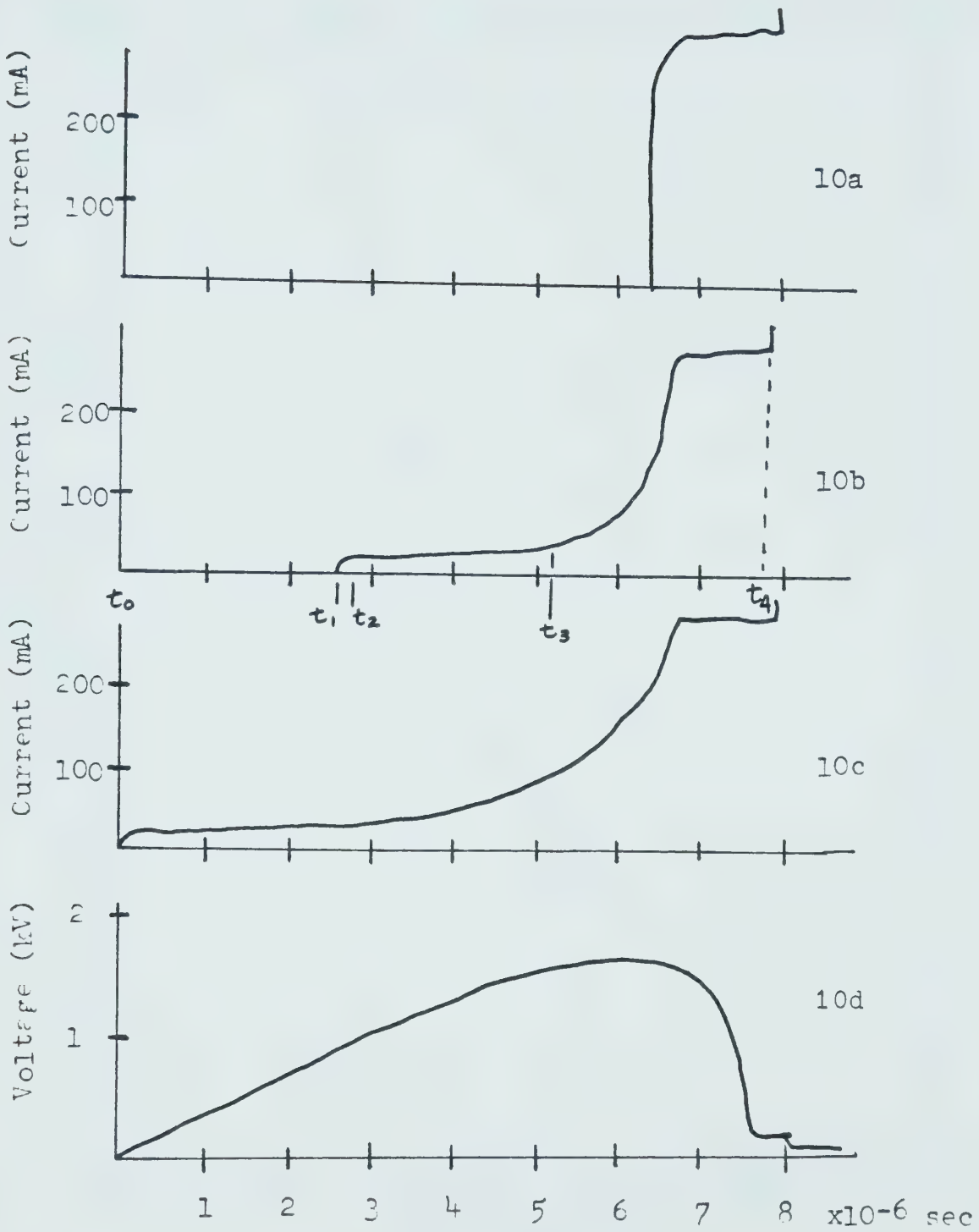

Figure 10. Current-voltage characteristic of breakdown in a flame.

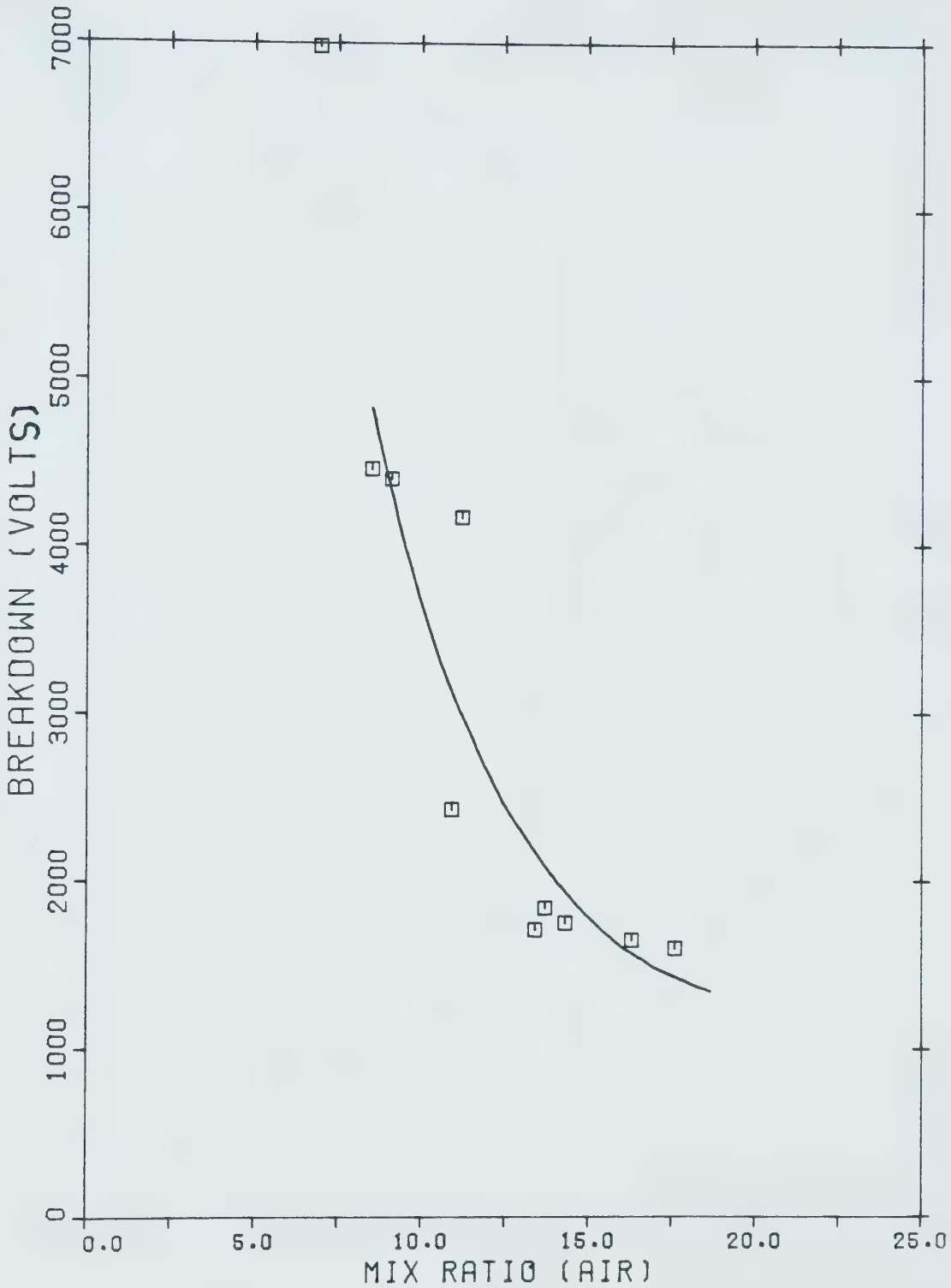

Figure 11. Breakdown voltage versus mixture ratio F_A/F_P.

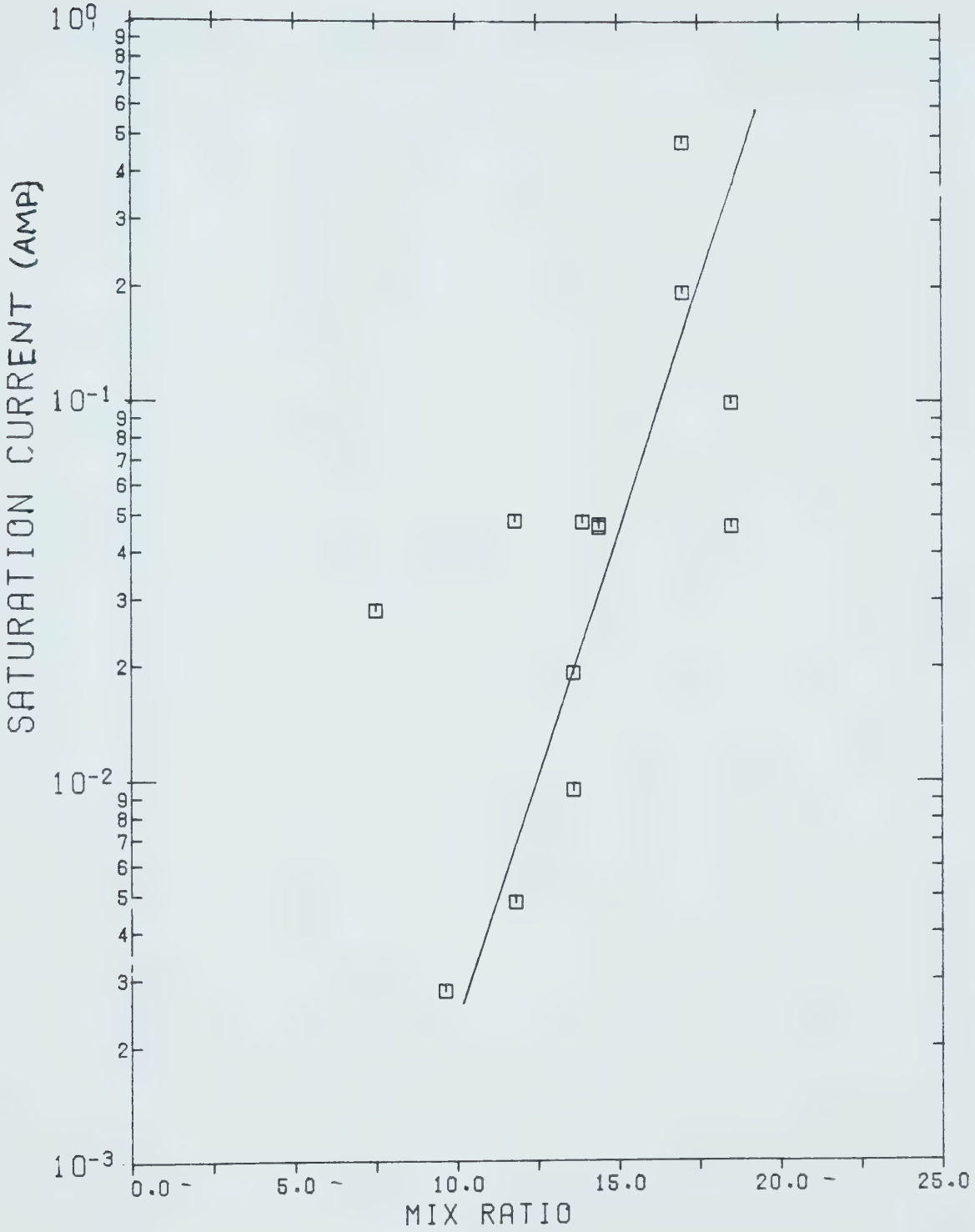

Figure 12. Calculated saturation current versus mixture ratio F_A/F_P.

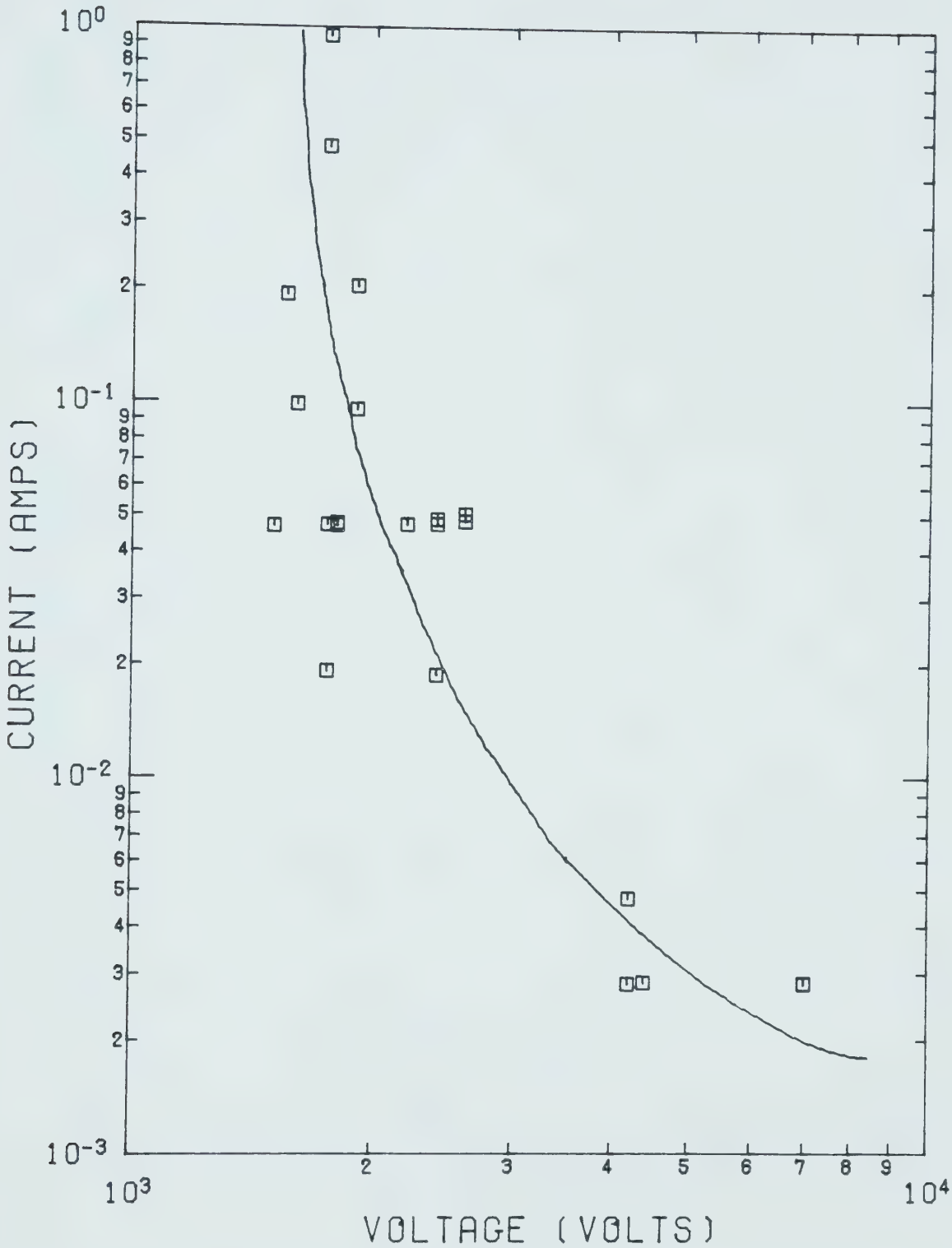

Figure 13. Breakdown voltage versus saturation current.

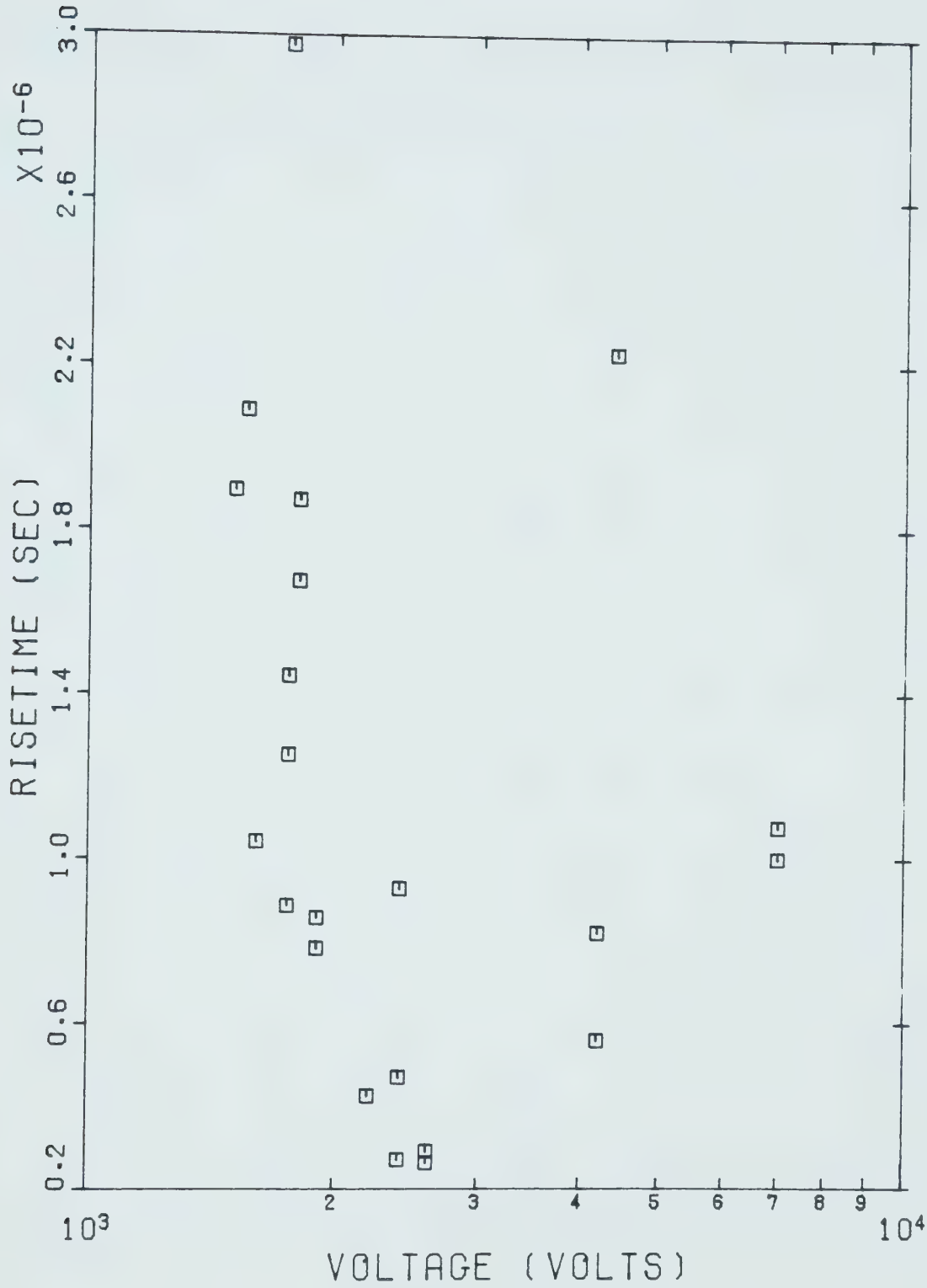

Figure 14. Breakdown voltage versus current risetime.

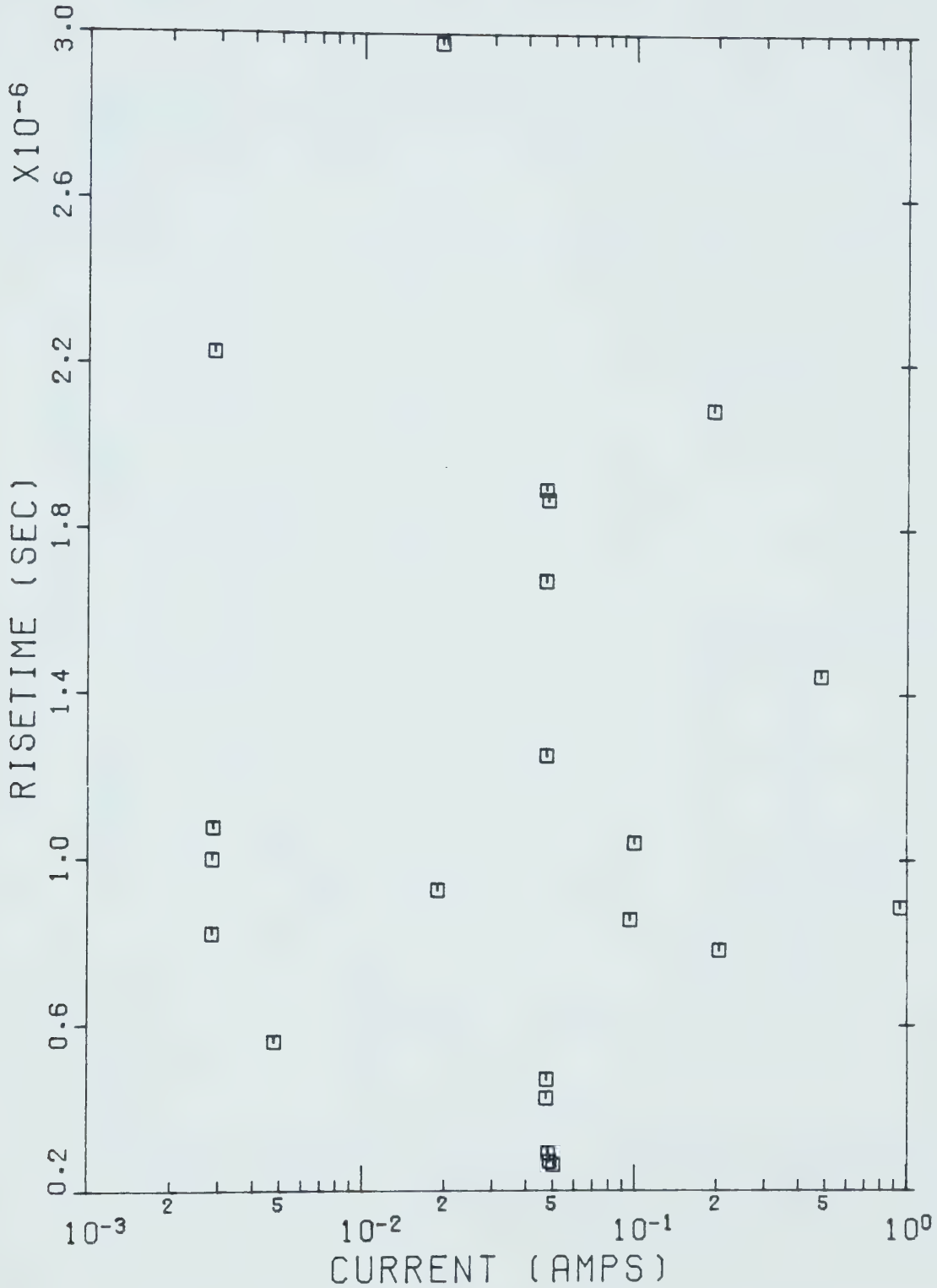

Figure 15. Saturation current versus current risetime.

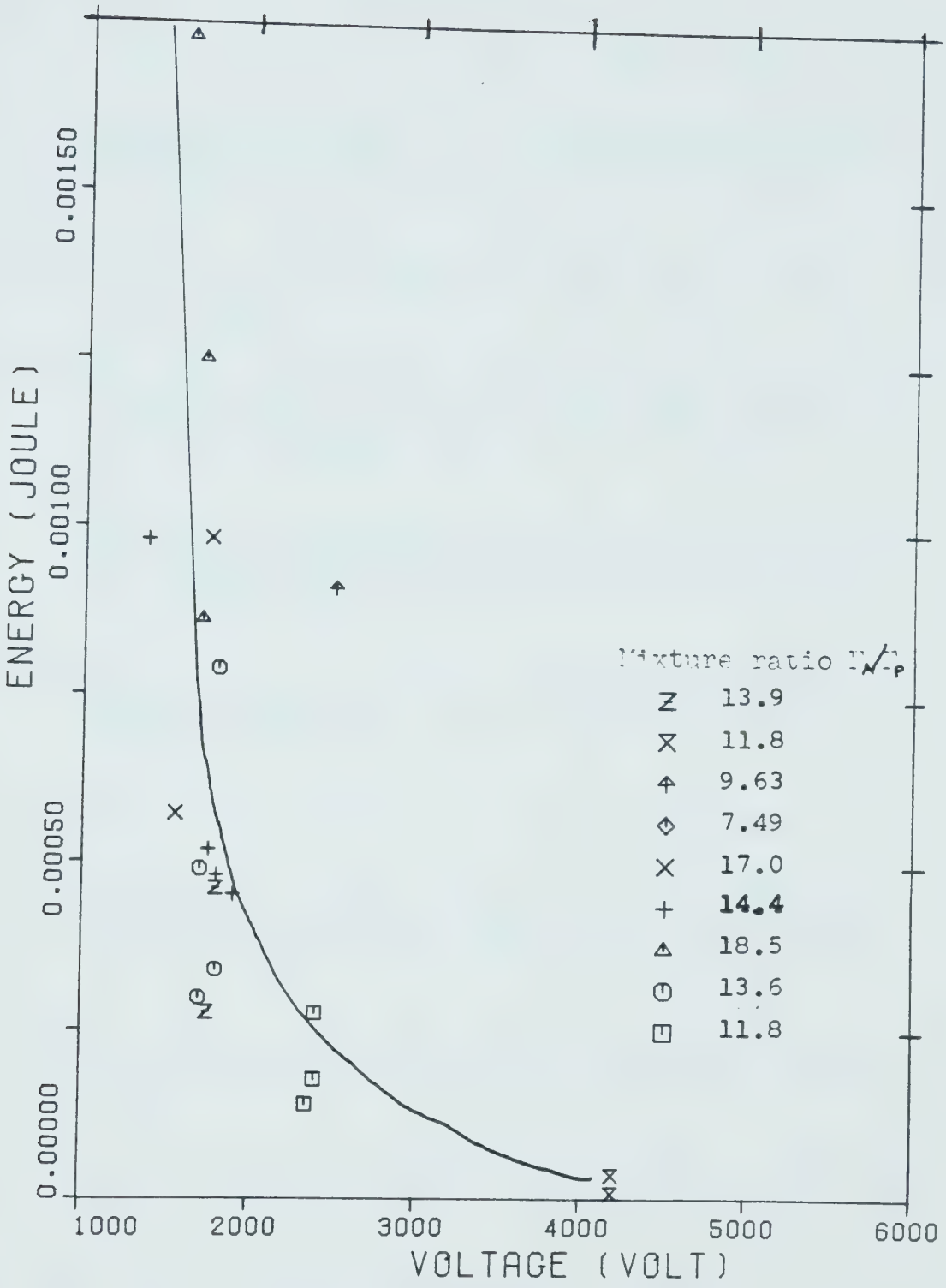

Figure 16. Input energy versus breakdown voltage.

BIBLIOGRAPHY

(1) Cam, John C.; Rose, Peter H.: " Electric Arc Driven Shock Tube ", Vol. 6, Physics of Fluids, pp. 663-678, 1963.

(2) Cho, M. S.: " Hot Plasma in Contact with a Cold Wall ", Physics of Fluids, Vol. 16, pp. 1441-1445, 1973.

(3) Clement, R. M.; Smy, P. R.: " The Effects of Ionization And Gas Flow On Spark Gap Recovery ", Journal of Physics D: Applied Physics, Vol. 6, pp. 1253-1265, 1973

(4) Clement, R. M.; Smy, P. R.: " Ion Current from a Collision Dominated Flowing Plasma to a Cylindrical Electrode Surronded by a Thin Sheath ", Journal of Applied Physics, Vol. 41, pp. 3745-3749, 1970.

(5) Flurscheim, C. H., editor: Power Circuit Breaker Theory and Design , Peter Peregrinus Ltd., England, 1975

(6) Haydon, S. C.: See Rees, J. A.: pp. 146-171.

(7) Greene, E. F. ; Hornig D. F. ; " The Shape and Thickness of Shock Fronts in Argon, Hydrogen, Nitrogen and Oxygen", The Journal of Chemical Physics, Vol. 21, No. 4, pp. 617-624, 1953.

(8) Gross, Robert A.: " Strong Ionizing Shock Waves ", Review of Modern Physics, Vol. 37, pp. 724-743, 1965.

(9) Llewellyn Jones, F.; Parker, A. B.: See Rees Pp. 54-70

(10) Kohrman, W.: See Rees, J. A., pp. 174-186.

(11) Lawton, J.; Weinberg F. J.: Electrical Aspects of Combustion , Clarendon Press, Oxford, 1969.

(12) Lawton, J.; Weinberg F. J.: " Maximum Ion Currents from Flames and Maximum Effects of Applied Electric Field ", Royal Society of London Series A, Vol. 277, pp. 468-497, 1964.

(13) Lee, T. H.; Greenwood, A. N.; White, D. R.: " Electrical Breakdown of High Temperature Gases and Its Implications in Post-Arc Phenomena in Circuit Breakers ", IEEE Transactions on Power Aparatus and Systems, Vol. PAS-84, pp. 1116-1125, 1965.

(14) Loeb, Leonard B.: Fundamental Processes of Electrical Discharge in Gases , John Wiley & Sons Inc., New York, 1939.

(15) Meek, J. M.: See Rees, J. A., pp. 42-51.

(16) Mikoshiba, S.; Smy, Peter R.: " Electrical Breakdown in a Collision Dominated Plasma ", Journal of Applied Physics, Vol. 44, pp. 1562-1570, 1973

(17) Mikoshiba, S.: Electrical Breakdown in a Plasma , PhD. Thesis, University of Alberta, 1971.

(18) Penning F. M.: Electrical Discharge in Gases , Cleaver Hume Press Ltd., W. C., 1965.

(19) Rees, J. A., editor: Electrical Breakdown in Gases , The MacMillan Press Ltd., London and Basingstoke, 1973.

(20) Resler, E. L.; Shao-Chi Lin; Kantrowitz A.: " Production of High Temperature Gases in Shock Tubes ", Journal of Applied Physics, Vol. 23, pp. 1390-1399, 1952.

(21) Saha, M. N.; Srivastava, B. N.: A Text Book Of Heat , The Indian Press Ltd., Allahabad(India), 1934. and Calcutta 1934.

(22) Sharbaugh, A. H.; Watson, P. K.; White, D. R.; Lee, T. H.; Greenwood, A.: " An Investigation of the Breakdown Strength of Nitrogen at High Temperatures ", IEEE Transactions of Power Apparatus and Systems, Vol. 80, pp. 333-344, 1961.

(23) Simpson, D.: Light Reflection from Shock Waves , PhD. Thesis, University of Alberta, 1970.

(24) Smy, P. R.: "The Uses of Langmuir Probes in the Study of High Pressure Plasmas", Advances in Physics, Vol. 25, pp. 517-553, 1976.

(25) VonEngel A. : Ionized Gases, Clarendon Press, Oxford,1965.

APPENDIX

Ramp circuit

Instead of taking discrete measurements, a continuously increasing voltage source was used due to the unstable nature of the breakdown mechanism. The waveform, though preferably linear for easy interpretation of results, was in fact exponential in nature. The rise time of the voltage also had to be slow enough to allow the ions to achieve equilibrium.

The waveform generator was originally to have been used in conjunction with the shock tube and it had been determined that 10 μs was the maximum time available for the voltage sweep.

The input voltage waveform to the probe was generated by a simple double capacitor discharge as illustrated in Fig. A1 . The capacitor C is charged to about 12 kV and then discharged into a simple RC network giving an exponentially increasing voltage with a time constant of about 17 μs. After peaking, the whole network then slowly discharges to zero over a relatively long time period. The RC network was made up of two oil filled capacitors (4 μF & 0.01 μF) and two Globar 350 Ω carbon composition resistor.

The output ramp was negative going with respect to ground and had a peak voltage of approximately 6.8 kV at t= 80 μs. There is an initial ringing of 1 kV but this was below the breakdown voltage of the flame and therefore was not thought to have significantly affected the resulting measurements.

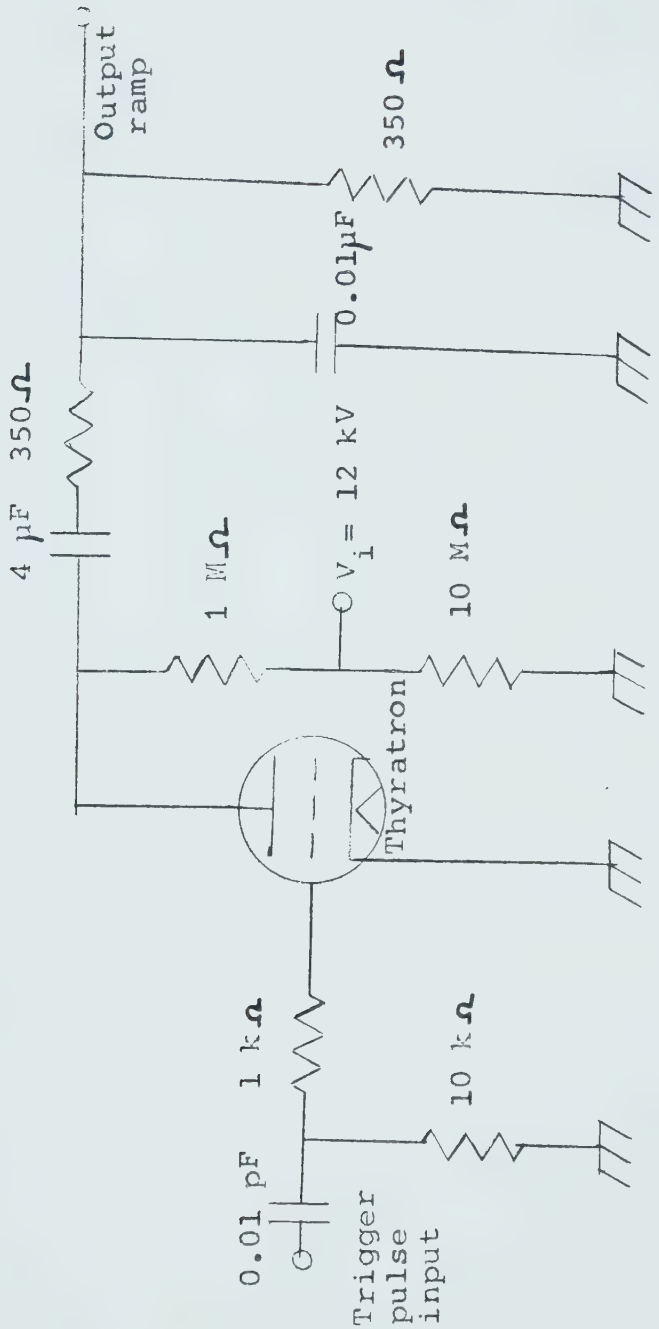

Figure A1. Ramp circuit.